Biochemistry and Biophysics Reports 9 (2017) 302–309

Contents lists available at ScienceDirect

Biochemistry and Biophysics Reports

journal homepage: www.elsevier.com/locate/bbrep

Adult human dermal fibroblasts exposed to nanosecond electrical pulses exhibit genetic biomarkers of mechanical stress

Caleb C. Roth[a,b,c,*], Randolph D. Glickman[d], Stacey L. Martens[c], Ibtissam Echchgadda[c], Hope T. Beier[e], Ronald A. Barnes Jr., [c], Bennett L. Ibey[c]

[a] University of Texas Health Science Center San Antonio, School of Medicine, Dept. of Radiological Sciences, 7703 Floyd Curl Drive, San Antonio, TX 78229, USA
[b] General Dynamics IT, 4141 Petroleum Road, JBSA Fort Sam Houston, TX 78234, USA
[c] Human Effectiveness Directorate, 711th Human Performance Wing, Air Force Research Laboratory, Radio Frequency Bioeffects Branch, Bioeffects Division, 4141 Petroleum Road, JBSA Fort Sam Houston, TX 78234, USA
[d] University of Texas Health Science Center San Antonio, School of Medicine, Dept. of Ophthalmology, 7703 Floyd Curl Drive, San Antonio, TX 78229, USA
[e] Human Effectiveness Directorate, 711th Human Performance Wing, Air Force Research Laboratory, Optical Radiation Bioeffects Branch, Bioeffects Division, 4141 Petroleum Road, JBSA Fort Sam Houston, TX 78234, USA

ARTICLE INFO

Keywords:
Adult human dermal fibroblasts
Mechanical stress
Microarray
Nanosecond electrical pulse
FOS
ITPKB

ABSTRACT

Background: Exposure of cells to very short (< 1 μs) electric pulses in the megavolt/meter range have been shown to cause a multitude of effects, both physical and molecular in nature. Physically, nanosecond electrical pulses (nsEP) can cause disruption of the plasma membrane, cellular swelling, shrinking and blebbing. Molecularly, nsEP have been shown to activate signaling pathways, produce oxidative stress, stimulate hormone secretion and induce both apoptotic and necrotic death. We hypothesize that studying the genetic response of primary human dermal fibroblasts exposed to nsEP, will gain insight into the molecular mechanism(s) either activated directly by nsEP, or indirectly through electrophysiology interactions.
Methods: Microarray analysis in conjunction with quantitative real time polymerase chain reaction (qRT-PCR) was used to screen and validate genes selectively upregulated in response to nsEP exposure.
Results: Expression profiles of 486 genes were found to be significantly changed by nsEP exposure. 50% of the top 20 responding genes coded for proteins located in two distinct cellular locations, the plasma membrane and the nucleus. Further analysis of five of the top 20 upregulated genes indicated that the HDFa cells' response to nsEP exposure included many elements of a mechanical stress response.
Conclusions: We found that several genes, some of which are mechanosensitive, were selectively upregulated due to nsEP exposure. This genetic response appears to be a primary response to the stimuli and not a secondary response to cellular swelling.
General significance: This work provides strong evidence that cells exposed to nsEP interpret the insult as a mechanical stress.

1. Introduction

Pulsed electrical discharges, in an aqueous medium, can cause a multitude of physical events to occur that, in turn, affect the biology of living things near the exposure area. Physical events such as: thermal-elastic expansion [1,2], electrostriction [3], electrochemistry [4] and plasma formation [3,5] can occur, if the correct exposure conditions are met. Thermal-elastic expansion depends on pulse duration, electrostriction occurs with high electric fields, electrochemistry is driven by high current and plasma formation dominates when there is break down within the exposure medium. Nanosecond electrical pulses (nsEP), a type of pulsed electrical discharge, are used in a variety of applications ranging from cancer therapy to food preservation [6,7]. The nsEP are too short to elicit a thermal response and typically do not form plasmas (at the voltages used for biological research). Research undertaken by our group suggests that electrostriction and electrochemistry may occur following nsEP and thus may be responsible in part for the biological effects associated with these exposures [unpublished personal communication].

Nanosecond electrical pulses have been shown to cause a wide variety of biological effects to cells, both morphological and biochemical in nature, These effects include swelling [8,9], blebbing [8,9],

* Corresponding author at: 711th HPW, Air Force Research Laboratory, 4141 Petroleum Road, Fort Sam Houston, TX 78234, USA.
E-mail address: calebcroth@gmail.com (C.C. Roth).

http://dx.doi.org/10.1016/j.bbrep.2017.01.007
Received 17 March 2016; Received in revised form 17 November 2016; Accepted 24 January 2017
Available online 25 January 2017
2405-5808/ Published by Elsevier B.V.

Table 1
nsEP parameters used for pulse ramp experiment.

Electric field	50 kV/cm	100 kV/cm	150 kV/cm
Number of pulses applied	10	10	10
	30	30	30
	100	100	100
	300	300	300
	1000	1000	1000

phospholipid translocation [9–12] and membrane permeabilization [11,13–15]. These morphological changes are closely associated with cell death and have been identified as markers of both apoptosis [8,16] or necrosis [8,16]. In addition to these phenomena, molecular/biochemical events such as the influx of calcium [17–20], the activation of the inositol triphosphate (IP_3) pathway [21–23], the creation of reactive oxygen species (ROS) [24–26] and the induction of autophagy [27] have also been reported as being associated with nsEP exposure.

Despite this wealth of biological evidence, very little is known about how nsEP affect gene expression in primary cells. Understanding how a cell interprets a stress can give great insight in the nature of the stress itself. Therefore, to better understand the nature of nsEP we performed a microarray analysis of a primary cell type exposed to nsEP. Human dermal fibroblasts (HDFa) are a primary cell, isolated from adult skin. These cells are considered to be "normal" with little genomic instability. These cells have also been used extensively in studies involving mechanical stress. Fibroblasts are often subjected to many different kinds of mechanical force, such as tension, compression and shear forces [28–30]. It has been reported that fibroblasts in a human tendon respond to stretching forces in a stretch-magnitude-dependent manner, where gene expression increases with stretch magnitude [30]. Given the ability of HDFa cells to not only regulate gene transcription based on specific types of mechanical stress, but also on the amplitude of that stress, we selected these cells to further investigate the mechanical stress imparted on cells by nsEP exposure. We exposed these cells to 100 nsEPs at a duration of 10-ns and an electric field of 150 kV/cm and assayed with microarray for global changes in gene expression 4 h post exposure. Quantitative Real-Time PCR was used to confirm the microarray data. The genomics data presented in this paper provide further genetic evidence necessary to characterize the nature of the stress endured by these cells when exposed to nsEP. This study represents the first global genetic analysis of normal human primary cells exposed to nsEP.

2. Materials and methods

2.1. Cell culture/exposure

Primary adult human fibroblast were acquired from Cascade Biologics (Carlsbad, CA), sub-cultured and maintained according to the supplier's protocol. Cells were grown in Medium 106 supplemented with a low serum growth supplement (LSGS) Kit, both purchased from Gibco (Carlsbad, CA). All cells were maintained at 37 °C/5% CO_2/95% humidity. The HDFa were prepared for exposure in accordance with

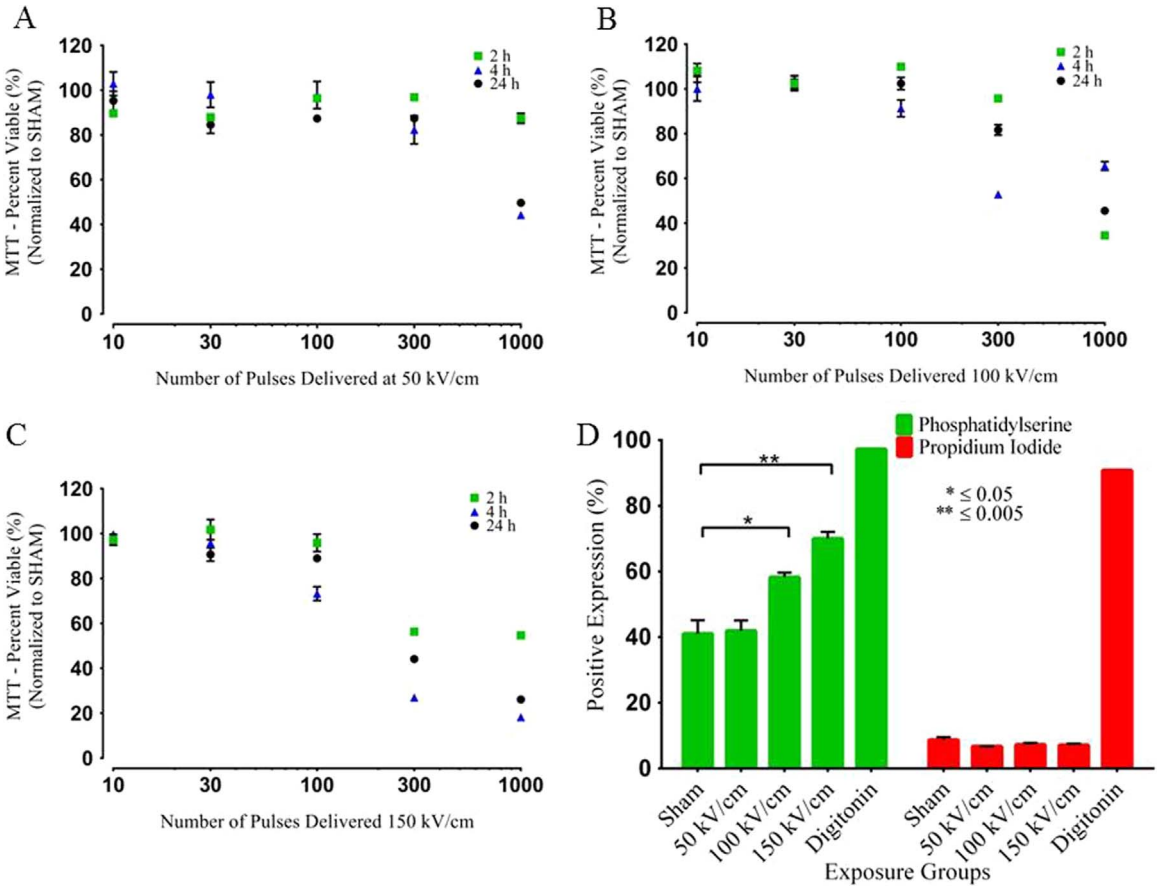

Fig. 1. Viability of HDFa after exposure to nsEP and normalized to SHAM. A) HDFa cells exposed to 10 ns duration pulses at an applied voltage of 50 kV at 1, 10, 30, 100, 300, or 1000 pulses at 1 Hz and at 2, 4 or 24 h post exposure. B) HDFa cells exposed to an applied voltage of 100 kV at 1, 10, 30, 100, 300, or 1000 pulses at 1 Hz and at 2, 4 or 24 h after exposure. C) HDFa cells exposed to an applied voltage of 150 kV at 1, 10, 30, 100, 300, or 1000 pulses at 1 Hz and at 2, 4 or 24 h after exposure. At 150 kV and at 100 pulses we achieved the desired level of viability. D) Flow cytometry data for phosphatidylserine (PS) and Propidium Iodide (PI) in cells exposed to 100 pulses at 50, 100, and 150 kV/cm electric fields. Cells exposed at 150 kV/cm and 100 pulses showed the highest level of membrane disruption (PS) with minimal death (PI). All experiments (flow cytometry and MTT) were performed in triplicate (3 independent nsEP exposures which were then divided into triplicate in each well plate for a total of 9 samples). A two-tailed unpaired t-test was performed using GraphPad Prism.

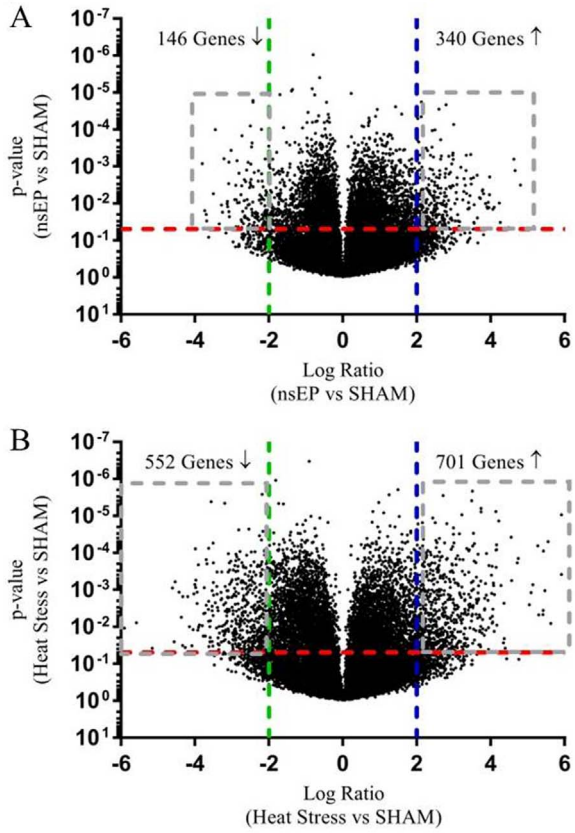

Fig. 2. Volcano plot of microarray data. Lines were inserted into the graph at a log ratio of +2 (blue) and −2 (green). An additional line (red) was inserted on the y-axis at a p-value of 0.05. Genes to the right of +2 (or left of −2) line and above the p-value line were considered to be significant. A) nsEP vs SHAM genetic profile plotted log ratio vs p-value (N=3). B) Heat stress (positive stress control) vs SHAM genetic response plotted p-value vs. log ratio. The Y-axis represents p-value in powers of 10. The gray outlined boxes represent genes with a log ratio of >2 or <-2 and a p-value of <0.05. (N=3).

the supplier's protocol. Cells were counted using the Countess® Cell Counter from Life Technologies (Grand Island, NY) and the final concentration was adjusted to 1200 cells/μL in complete growth medium. The cells were then aliquoted into 1 mm gap (150 μL volume) electroporation cuvettes (VWR, Radnor, PA) and were exposed to either nsEP or they were SHAM exposed (both in complete growth medium) [31]. SHAM and nsEP exposures occurred in a random fashion. The SHAM control samples were treated identically to the nsEP exposed samples except, when they were placed on the pulser, zero power was applied. To determine the appropriate pulse parameters for microarray analysis, a pulse ramp was performed at 50, 100, and 150 kV/cm (Table 1). The nsEP exposures for microarray analysis were 100, 10 ns electrical pulses at 150 kV/cm. All pulses were delivered at a rate of 1 Hz. Following either SHAM or nsEP exposure, the cells were transferred into a well plate in triplicate and incubated in the appropriate cell culture conditions for the allotted time necessary for each assay. In an effort to gauge the genetic response to nsEP, cells were subjected to a known heat stress protocol [32]. The heat shocked thermal control samples were placed in identical electroporation cuvettes and incubated in a circulating water bath at 44 °C for 40 min. The 10-ns exposure system used in this study has been previously described [33,34].

2.2. MTT Assay

Viability was evaluated at 2, 4, and 24 h post exposure using MTT (3-(4,5-dimethylthiazol-2-yl)−2,5-diphenyltetrazolium bromide) assay, as per the manufacturer's instructions (ATCC, Manassas, VA). In brief, cells were exposed to nsEP and incubated for 0, 2 or 22 h, and then 10 μL of MTT reagent (ATCC) was added to each well. For the 2 h time point, MTT reagent was added immediately after exposure. After the addition of the MTT reagent to each time point, cells were incubated at 37 °C/5% CO_2/95% humidity for 2 h until the formazan precipitate was visible. Then, 100 μL of detergent was added to each well and the plate was covered in foil, placed on an orbital shaker at 100 rpm and incubated at room temperature overnight. The absorbance was then measured at 570 nm with a Synergy HT Plate Reader (BioTek©, Winooski, VT).

2.3. Cell flow cytometry

Cells were prepared and exposed identically as in cell survival experiments. Immediately after exposure, FITC-Annexin V (PS) which labels phosphatidylserine, and Propidium Iodide (PI) which labels nucleic acids (Invitrogen, Grand Island, NY) were added at 10 μL/mL and 2 μL/mL concentrations, respectively. The cells were then allowed to incubate in the exposure media with the above mentioned dyes at room temperature (26 °C) for 10 min and were assayed on the Accuri Flow Cytometer from BD Biosciences (San Jose, California) immediately after incubation. A total volume of 75 μL of media was analyzed resulting in typical cellular counts of ~40,000 cells. Fluorescence was normalized for each individual channel using SHAM exposure (negative control) and 0.1% Digitonin (Sigma-Aldrich, St. Louis, MO) exposure (positive control). A single threshold was determined and the percentage of cells expressing each dye was measured. A two-tailed unpaired *t*-test was performed using GraphPad Prism. In addition to the fluorescence data collected, both side scattering and forward scattering data was recorded for each cell.

2.4. Ribonucleic acid (RNA) isolation

Total RNA was isolated from exposed cells and harvested 4 h post exposure. This RNA was both used for microarray analysis as well as PCR validation. RNA was isolated using the Qiagen RNeasy Mini Kit and subjected to DNase digestion by the Qiagen RNase-free DNase Kit (QIAGEN Inc. Valencia, CA). RNA quantity was assessed by UV spectrometry at 260 nm/280 nm absorbance on the NanoDrop Spectrophotometer (NanoDrop Technologies, Wilmington, DE). RNA quality was assessed on the Agilent Bioanalyzer using the Agilent RNA Nano Chips (Agilent Technologies, Waldbronn, Germany).

2.5. Microarray

Expression analysis was performed for each experimental group in triplicate (three control, three nsEP exposed and three heat-shock treated samples) using the Affymetrix GeneChip® Human Genome U133 (HG-U133) plus 2.0 array (Affymetrix, Santa Clara, California) that contains 54,675 probe sets. Samples were analyzed according to the manufacturer's suggested protocol. Image signal data, detection calls and annotations were generated for every gene using the Affymetrix Statistical Algorithm MAS 5.0 (GeneChip® Operating Software version 1.3). A log2 transformation was conducted and a Student's t-test was performed for comparison of the two groups (control and heat-shocked). We conducted multiple testing correction—Benjamini and Hochberg—to determine the false discovery rate, and statistically significant genes were identified using Bonferroni correction procedures. For interpretation of the results, Ingenuity Pathways Analysis (IPA) tool (IPA version 8.7, Ingenuity® Systems Inc., Redwood City, CA) was used. The cut-off criteria for our IPA analysis were an absolute value of log2 ratio ≥2.0 and a p-value ≤0.05. Other web-based resources, such as the NCBI Gene Ontology database, were also used to further supplement the analysis.

Table 2
Top 20 upregulated genes and top 20 down-regulated genes.

Symbol	Gene name	Gene ID	Log ratio	Fold change	p-Value
Upregulated					
FOS	FBJ murine osteosarcoma viral oncogene homolog	2353	4.801	27.88	3.18E−03
ITPKB	inositol-trisphosphate 3-kinase B	3707	4.659	25.26	1.29E−03
POSTN	periostin, osteoblast specific factor	10631	4.623	24.64	6.35E−04
GREB1	growth regulation by estrogen in breast cancer 1	9687	4.477	22.27	4.48E−02
KLHL24	kelch-like family member 24	54800	4.228	18.74	9.78E−03
NR4A2	nuclear receptor subfamily 4, group A, member 2	4929	4.059	16.67	1.43E−02
SOD2	superoxide dismutase 2, mitochondrial	6648	3.972	15.697	1.92E−03
OR7C1	olfactory receptor, family 7, subfamily C, member 1	26664	3.803	13.96	5.48E−03
CLDN23	claudin 23	137075	3.719	13.17	7.25E−03
PROK2	prokineticin 2	60675	3.678	12.80	4.65E−02
FGFR1OP2	FGFR1 oncogene partner 2	26127	3.632	12.40	1.71E−03
ARID4B	AT rich interactive domain 4B (RBP1-like)	51742	3.548	11.70	3.39E−02
TFEC	transcription factor EC	22797	3.548	11.70	1.10E−02
UNC13C	unc−13 homolog C (*C. elegans*)	440279	3.546	11.68	3.22E−02
HCN1	hyperpolarization activated cyclic nucleotide-gated K^+ channel 1	348980	3.53	11.55	2.01E−03
FCRL1	Fc receptor-like 1	115350	3.458	10.99	4.72E−04
GPC5	glypican 5	2262	3.437	10.83	6.20E−03
PIAS2	protein inhibitor of activated STAT, 2	9063	3.415	10.67	1.33E−02
ARHGEF12	Rho guanine nucleotide exchange factor (GEF) 12	23365	3.382	10.43	1.41E−02
LRP1	low density lipoprotein receptor-related protein 1	4035	3.334	10.08	4.99E−04
Down-Regulated					
UNC5C	unc−5 homolog C (C. elegans)	8633	−2.662	−6.33	2.29E−03
C17orf70	chromosome 17 open reading frame 70	80233	−2.732	−6.64	1.47E−04
DNAH5	dynein, axonemal, heavy chain 5	1767	−2.754	−6.75	5.83E−03
PCYT1B	phosphate cytidylyltransferase 1, choline, beta	9468	−2.848	−7.20	9.69E−03
USP21	ubiquitin specific peptidase 21	27005	−2.86	−7.26	6.94E−04
KIF7	kinesin family member 7	374654	−2.923	−7.58	7.94E−03
PYGB	phosphorylase, glycogen; brain	5834	−3.024	−8.13	3.66E−04
RNASEL	ribonuclease L (2′,5′-oligoisoadenylate synthetase-dependent)	6041	−3.073	−8.42	2.29E−02
KCNS2	K^+ voltage-gated channel, subfamily S, member 2	3788	−3.082	−8.47	7.61E−04
DUOX1	dual oxidase 1	53905	−3.086	−8.49	1.66E−02
HIPK2	homeodomain interacting protein kinase 2	28996	−3.091	−8.52	2.89E−03
ZNF287	zinc finger protein 287	57336	−3.116	−8.67	1.23E−02
CADM2	cell adhesion molecule 2	253559	−3.124	−8.72	8.78E−03
FUT6	fucosyltransferase 6 (alpha (1,3) fucosyltransferase)	2528	−3.129	−8.75	1.02E−02
N6AMT1	N−6 adenine-specific DNA methyltransferase 1 (putative)	29104	−3.214	−9.28	6.16E−04
SPATA9	spermatogenesis associated 9	83890	−3.253	−9.53	1.73E−02
PRMT7	protein arginine methyltransferase 7	54496	−3.284	−9.74	1.11E−02
PYCRL	pyrroline−5-carboxylate reductase-like	65263	−3.346	−10.17	3.54E−02
NSD1	nuclear receptor binding SET domain protein 1	64324	−3.448	−10.91	1.01E−04
CWF19L2	CWF19-like 2, cell cycle control	143884	−3.696	−12.96	1.97E−02

2.6. Quantitative Real-Time PCR

Each gene selected for validation was corroborated by quantitative Real-Time PCR (qRT-PCR) using the Applied Biosystems StepOne™ Plus PCR system from Life Technologies. Pre-made, validated TaqMan® Gene Expression Assays were selected for each gene to be validated. Samples were run in triplicate with all reagents from Life Technologies, including the TaqMan® One-Step RT-PCR Master Mix. Relative quantification (RQ) values were computed using the StepOne™ Plus software.

3. Results

3.1. Viability

Prior to isolating RNA for genetic analysis, the optimum exposure parameters and time point for eliciting a stress response from the HDFa cells was determined. Exposure parameters performed on the cells, for the microarray analysis, were chosen based on parameters that yielded approximately 70% viability, indicating a sub-lethal exposure where at least 2/3 of the exposed cells survived. We found that HDFa cells were quite resistant to the effects of nsEP. Very little death was observed with an applied field of 50 kV/cm; only at 1000 pulses were we able to achieve appreciable death (Fig. 1A). With an electric field of 100 kV/cm, 70% viability was not achieved (Fig. 1B). At 100 kV/cm, 100 pulses did not produce enough death and 300 pulses produced too much death. With an electric field of 150 kV/cm, we were able to achieve the desired level of approximately 70% viability with 100 pulses and at a time point of 4 h post exposure (Fig. 1C). We selected 100, 10-ns pulses, at an applied field of 150 kV/cm, as our exposure parameters, and 4 h post exposure as our time point for our genetics study. Flow cytometry data (Fig. 1D) confirmed that at 150 kV/cm the membranes of the HDFa cells were the most perturbed, as indicated by the increased expression of phosphatidylserine (PS). At the highest electric field (150 kV/cm), PI expression was minimal, indicating very little necrotic death and/or large molecule permeabilization occurred.

3.2. Microarray analysis

The expression profile of the nsEP samples was compared to the expression profile of the SHAM samples; from this comparison, a log ratio and p-value were calculated for each gene. This process was repeated for the thermal control group. Looking for the greatest genetic response, we eliminated all of the genes that did not show a log ratio of > 2 or < -2 and a p-value greater than 0.05. Following these guidelines 486 genes, selectively up- or down-regulated by nsEP exposure, remained. Volcano plots using the log ratio of each gene with its

Table 3
Products of the Top 20 Upregulated and the Top 20 Down-regulated Genes: Location within the cell and the type of protein.

Symbol	Location	Type
FOS	Nucleus	transcription regulator
ITPKB	Cytoplasm	kinase
POSTN	Extracellular Space	other
GREB1	Cytoplasm	other
KLHL24	Other	other
NR4A2	Nucleus	ligand-dependent nuclear receptor
SOD2	Cytoplasm	enzyme
OR7C1	Plasma Membrane	G-protein coupled receptor
CLDN23	Plasma Membrane	other
PROK2	Extracellular Space	other
FGFR1OP2	Cytoplasm	other
ARID4B	Nucleus	other
TFEC	Nucleus	transcription regulator
UNC13C	Cytoplasm	other
HCN1	Plasma Membrane	ion channel
FCRL1	Other	other
GPC5	Plasma Membrane	other
PIAS2	Nucleus	transcription regulator
ARHGEF12	Cytoplasm	other
LRP1	Plasma Membrane	transmembrane receptor
UNC5C	Plasma Membrane	transmembrane receptor
C17orf70	Nucleus	other
DNAH5	Cytoplasm	enzyme
PCYT1B	Cytoplasm	enzyme
USP21	Cytoplasm	peptidase
KIF7	Extracellular Space	other
PYGB	Cytoplasm	enzyme
RNASEL	Cytoplasm	enzyme
KCNS2	Plasma Membrane	ion channel
DUOX1	Plasma Membrane	enzyme
HIPK2	Nucleus	kinase
ZNF287	Nucleus	transcription regulator
CADM2	Plasma Membrane	other
FUT6	Cytoplasm	enzyme
N6AMT1	Other	enzyme
SPATA9	Other	other
PRMT7	Cytoplasm	enzyme
PYCRL	Other	enzyme
NSD1	Nucleus	transcription regulator
CWF19L2	Other	other

associated p-value are shown in Fig. 2. Lines were inserted into the graph at a log ratio of +2 (blue) and −2 (green). An additional line (red) was inserted on the y-axis at a p-value of 0.05. Genes to the right of the +2 line, or left of the −2 line, and above the p-value line were considered to be significant. The thermal stress protocol elicited a genetic response with more than double the number of responding genes that was observed in the nsEP exposure set (1253 genes vs 486 genes). The microarray data discussed in this publication have been deposited in NCBI's Gene Expression Omnibus and are accessible through GEO Series accession number GSE77906 (http://www.ncbi.nlm.nih.gov/geo/query/acc.cgi?acc=GSE77906).

3.3. IPA analysis

The 486 genes, identified by the filtering approach, were uploaded into Ingenuity Pathway Analysis (IPA) Software for further analysis. IPA software is a very powerful tool that can provide information about pathways associated with specific gene expression profiles as well as mine databases to provide information about location, function and upstream regulators of the changing genes. The 40 genes with the highest and lowest log ratios and with p-values < 0.05 appear in Table 2. Of the top 20 upregulated genes, 25% code for proteins located in the plasma membrane. Many of these proteins are transmembrane receptors or G-protein coupled receptors (Table 3). Furthermore, another 25%, of the top 20 upregulated genes code for proteins which typically localize to the nucleus. Thus, 50% of the top responding genes code for proteins located in two distinct cellular locations where nsEP exposure is thought to have its greatest effect. Of the top 20 down-regulated genes, seven genes code for proteins located in the cytoplasm and 10 genes code for enzymes. The location and function of the top responding genes can give insight into the nature of pathways affected by nsEP exposure.

3.4. qRT-PCR validation

Microarray expression was validated for 5 genes indicated by microarray analysis as being significantly upregulated with respect to nsEP exposure: FBJ Murine Osteosarcoma Viral Oncogene Homolog (FOS); Nuclear Receptor Subfamily 4, Group A, Member 2 (NR4A2); Inositol-Trisphosphate 3-Kinase B (ITPKB); Kelch-Like Family Member 24 (KLHL24) and Superoxide Dismutase 2, Mitochondrial (SOD2). Fig. 3 displays scatter dot plots with the mean (green line) and standard deviation (black line) for each qRT-PCR validation.

FOS and NR4A2 mRNA expression levels were significantly increased as compared to the SHAM (Fig. 3A,B); average fold changes (increase) of approximately 57 (range 29–112) and 41 (range 7 – 103) were observed, respectively. ITPKB and KLHL24 mRNA expression levels were moderately upregulated as compared to the SHAM (Fig. 3C, D); average fold changes of approximately 8 and 7 were observed, respectively. Finally, SOD2 mRNA expression levels were shown to be slightly increased as compared to the SHAM (Fig. 3E); an average fold change of 1.7 was observed.

3.5. Cellular swelling

To determine if the mechanical stress stimulus was due to cellular swelling, we analyzed the forward scattering (FSC-H) data collected from the flow cytometry analysis. Fig. 4 shows the mean FSC-H, in arbitrary units, for each triplicate sample. The blue lines represent the mean and the black lines represent the standard error of the mean. The mean FSC-H value for the SHAM samples was 3.19E+06. For the nsEP sample groups, 35, 50, 100 and 150 kV/cm, the mean FSC-H values were: 3.05E+06, 3.12E+06, 2.94E+06 and 2.77E+06 respectively, indicating no significant increase in cell size at 15 min post exposure; thus no swelling occurred. Cellular size did not increase, but rather decreased, after exposure, with the highest exposure displaying $< 10\%$ decrease in size.

4. Discussion

In our previous research, we have shown that nsEP can cause the generation of acoustic shock waves [35]. We found that these shock waves were most likely not directly responsible for nanoporation; however, we hypothesized that they might be strong enough to elicit a mechanical stress response. We performed a microarray analysis on both Jurkat and U937 cells exposed to nsEP and identified genetic markers of mechanical stress [31]. However, these cell types are not generally used in mechanobiological research; therefore the experiments were repeated with cells used in mechanobiology.

HDFa cells are well studied and are often used in mechanobiological research where stretch forces are applied; their genetic response to mechanical stress is well documented [30]. HDFa cells can withstand great mechanical stress due to their extensive cytoskeletal network [28,30]. However, their response to nsEP was unknown before this work. The results of this study revealed that HDFa cells are quite resistant to the effects of nsEP. At 150 kV/cm exposure HDFa cells showed little death, even at 1000 pulses. With 100 pulses delivered at 150 kV/cm, over 75% of cells expressed some level of membrane disruption while few cells died (as indicated by PS and PI expression in flow cytometry).

It is difficult to distinguish between actual mechanical stress (either external or internal) and membrane disruption which in itself could be

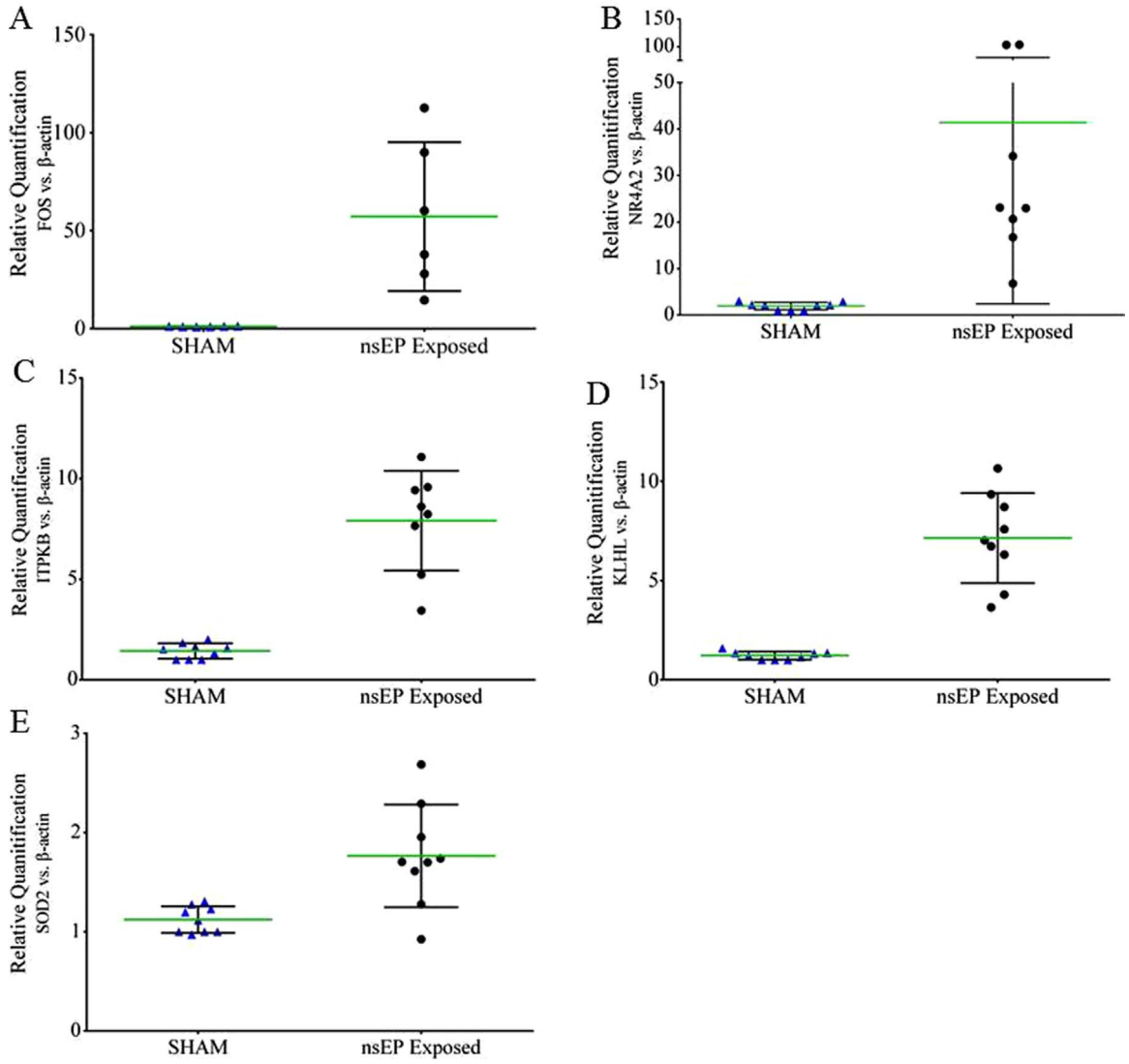

Fig. 3. Scatter dot plot with mean (green line) and standard deviation (black line) for each qRT-PCR validation sample. Relative expression levels indicated for the following HDF(a) genes at 4 h post exposure to nsEP: A) FOS. B) NR4A2. C) ITPKB. D) KLHL24. E) SOD2. RNA was isolated from each of the 3 independent exposures from each experimental group. This RNA was then assayed 3 times for at total of 9 assays for each experimental group.

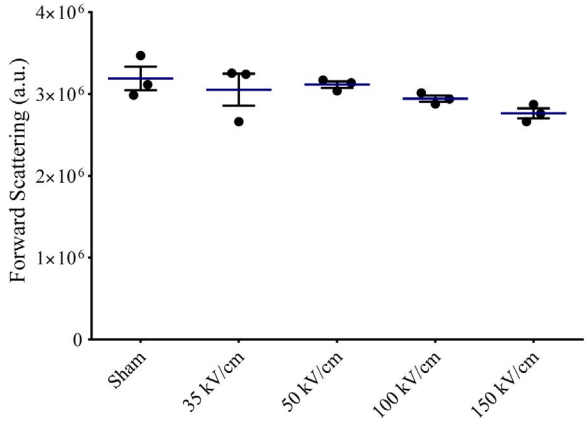

Fig. 4. Interleaved scatter plot of the mean forward scattering (FSC-H) of each exposure group (each of the 3 independent exposures was assayed in triplicate. The black dots represent the mean value for each independent exposure). The black lines represent the standard error of the mean. The blue line represents the mean of the triplicates.

interpreted as the byproduct of mechanical stress. Nanosecond electrical pulse exposures characteristically cause membrane disruption. Markers of membrane disruption that can also be interpreted as mechanical stress have been observed following nsEP exposure. These markers include: calcium release from the endoplasmic reticulum [36], disruption of the extracellular matrix and cytoskeleton [37–40], increased IP3 production [36], increases in GPCR and MAPK pathway signaling [41–44] and the production of ROS resulting in oxidative stress [45]. Each of these markers can be directly and indirectly linked to specific changes in gene expression.

Although gene expression analysis is a very powerful tool in identifying such things as how a cell responds to a particular insult, it cannot specifically identify that insult. Gene expression analysis tells researchers how a cell interprets the insult. Microarray analysis of the HDFa cells exposed to 100, 10 ns pulses at 150 kV/cm indicated that approximately 500 genes were significantly changed in response to nsEP. Analysis of five of the top 20 upregulated genes indicated that the HDFa cells' response to nsEP exposure included many elements characteristic of a mechanical stress response, however it cannot be determined if the disruption of the plasma membrane is either directly or indirectly responsible for this change in gene expression. The most significantly upregulated gene, FOS, displayed a log ratio of 4.8 (fold

change of 27.9). Although FOS plays many different roles associated with a generalized stress response, it is intriguing that it is the most upregulated gene in our nsEP samples, because it codes for a transcriptional regulator protein that ultimately localizes to the nucleus and is upregulated in response to increased mechanical stress [46,47].

Other genes known to be directly associated with mechanical stress, (as well as other stressors) were also upregulated in the nsEP exposed samples. NR4A2, a nuclear receptor gene, is known to be induced by mechanical agitation [48]. NR4A2 was highly upregulated with a log ratio of 4 (fold change of 16.7) in response to nsEP. Both FOS and NR4A2 mRNA expression were validated by qRT-PCR with median fold changes of 57 and 41, respectively. Hence, the genes most affected in this study, FOS and NR4A2, are both related to a mechanical stress response and are both sharply upregulated in nsEP exposed cells. This genetic up-regulation is consistent with what one would expect to find with cells exposed to a mechanical stress.

The gene inositol-trisphosphate 3-kinase B (ITPKB) is upregulated (log ratio 4.6; fold change of 25.3) in response to nsEP. ITPKB is a potent regulator of IP3 metabolism and has been shown to be essential for the propagation of rapid calcium waves emanating from the site of injury in wound healing [49]. ITPKB has also been shown to play an important role in cytoskeleton remodeling, specifically mobilization of F-actin. Two well-known genetic markers of oxidative stress, KLHL24 and SOD2 are also upregulated in response to nsEP exposure. Increases in SOD2 transcription have been directly linked to a specific antioxidative response induced by mechanical stretch [50].

The genetic profile generated in this study for adult human dermal fibroblasts exposed to nsEP contains a large amount of genetic evidence for our hypothesis that mechanical stress is one of the multiple stressors, if not the dominant stress, for these types of exposures. We hypothesize that mechanical stress imparted on the cell is due to a physical event occurring with the application of the electrical pulse. Although sucrose was not added to control for swelling, we analyzed cell size post exposure and compared that to the SHAM samples and saw little difference. Therefore, we postulate that cellular swelling was not the primary cause for the up-regulation in mechanosensitive genes.

Each of the top responding genes listed above has been shown to play a direct role in mechanical transduction, or an indirect role in the cellular response to mechanical stress. However, it is extremely difficult to differentiate between genes upregulated due to mechanical stress and/or to membrane disruption. The genetic data identified here suggests mechanical stress is responsible for the expression profile we have identified; however, we cannot rule out the possibility that there are likely multiple biophysical interactions other than mechanical stress occurring that could also contribute to this particular gene expression profile. Understanding the physical source responsible for this specific gene profile will be paramount to further research in the field of nsEP. Additional work will be undertaken to measure/characterize the magnitude of the pressure imparted by nsEP exposure in the cuvette-based setup. Taken all together, the findings presented in this paper provide evidence that mechanical stress could be experienced by cells exposed to nsEP and that the observed bioeffects associated with nsEP are likely due to mechanical perturbation.

Competing financial interests

The authors declare no competing financial interest.

Acknowledgements

We wish to thank the SMART Program (Grant no. N002440910081) Office of Secretary Defense-Test and Evaluation, Defense-Wide / PE0601120D8Z National Defense Education Program / BA-1, Basic Research and the Air Force Research Laboratory for providing us with the opportunity to conduct this study. This study was also supported by a grant from the Air Force Office of Scientific Research (Grant no. LRIR 16RHCOR348).

Appendix A. Transparency document

Transparency document associated with this article can be found in the online version at http://dx.doi.org/10.1016/j.bbrep.2017.01.007.

References

[1] J. Teissie, M. Golzio, M. Rols, Mechanisms of cell membrane electropermeabilization: a minireview of our present (lack of?) knowledge, Biochim. Et. Biophys. Acta Gen. Subj. 1724 (2005) 270–280.
[2] L. Wasungu, F. Pillet, E. Bellard, M.-P. Rols, J. Teissié, Shock waves associated with electric pulses affect cell electro-permeabilization, Bioelectrochemistry 100 (2014) 36–43.
[3] Y. Seepersad, M. Pekker, M.N. Shneider, D. Dobrynin, A. Fridman, On the electrostrictive mechanism of nanosecond-pulsed breakdown in liquid phase, J. Phys. D. Appl Phys. 46 (2013) 162001 Available: ⟨http://stacks.iop.org/0022-3727/46/i=16/a=162001⟩.
[4] A. Kraft, Electrochemical water disinfection: a short review, Platin. Met. Rev. 52 (2008) 177–185.
[5] M. Klas, S. Matejvcik, M. Radmilovic-Radjenovic, B. Radjenovic, Electrical breakdown and volt-ampere characteristics in water vapor in microgaps, EPL (Europhys. Lett.) 99 (2012) 57001.
[6] K.H. Schoenbach, S. Katsuki, R.H. Stark, E.S. Buescher, S.J. Beebe, Bioelectrics-new applications for pulsed power technology, IEEE Transactions Plasma Sci. 30 (2002) 293–300.
[7] M. Breton, L.M. Mir, Microsecond and nanosecond electric pulses in cancer treatments, Bioelectromagnetics 33 (2012) 106–123.
[8] O.N. Pakhomova, B.W. Gregory, I. Semenov, A.G. Pakhomov, Two modes of cell death caused by exposure to nanosecond pulsed electric field, PLoS One 8 (2013) e70278.
[9] R.L. Vincelette, C.C. Roth, M.P. McConnell, J.A. Payne, H.T. Beier, et al., Thresholds for phosphatidylserine externalization in Chinese hamster ovarian cells following exposure to nanosecond pulsed electrical fields (nsPEF), PLoS One 8 (2013) e63122.
[10] P.T. Vernier, Y. Sun, L. Marcu, C.M. Craft, M.A. Gundersen, Nanoelectropulse-induced phosphatidylserine translocation, Biophys. J. 86 (2004) 4040–4048.
[11] P.T. Vernier, Y. Sun, M. Gundersen, Nanoelectropulse-driven membrane perturbation and small molecule permeabilization, BMC Cell Biol. 7 (2006) 37.
[12] P.T. Vernier, Y. Sun, L. Marcu, C.M. Craft, M.A. Gundersen, Nanosecond pulsed electric fields perturb membrane phospholipids in T lymphoblasts, FEBS Lett. 572 (2004) 103–108. http://dx.doi.org/10.1016/j.febslet.2004.07.021.
[13] B.L. Ibey, D.G. Mixon, J.A. Payne, A. Bowman, K. Sickendick, et al., Plasma membrane permeabilization by trains of ultrashort electric pulses, Bioelectrochemistry 79 (2010) 114–121.
[14] A.G. Pakhomov, R. Shevin, J.A. White, J.F. Kolb, O.N. Pakhomova, et al., Membrane permeabilization and cell damage by ultrashort electric field shocks, Arch. Biochem. Biophys. 465 (2007) 109–118.
[15] A.G. Pakhomov, J.F. Kolb, J.A. White, R.P. Joshi, S. Xiao, et al., Long-lasting plasma membrane permeabilization in mammalian cells by nanosecond pulsed electric field (nsPEF), Bioelectromagnetics 28 (2007) 655–663. http://dx.doi.org/10.1002/bem.20354.
[16] L.E. Estlack, C.C. Roth, G.L. Thompson III, W.A. Lambert III, B.L. Ibey, Nanosecond pulsed electric fields modulate the expression of Fas/CD95 death receptor pathway regulators in U937 and jurkat cells, Apoptosis 19 (2014) 1755–1768.
[17] I. Semenov, S. Xiao, O.N. Pakhomova, A.G. Pakhomov, Recruitment of the intracellular Ca^{2+} by ultrashort electric stimuli: the impact of pulse duration, Cell Calcium 54 (2013) 145–150. http://dx.doi.org/10.1016/j.ceca.2013.05.008.
[18] S. Wang, J. Chen, M.-T. Chen, P.T. Vernier, M.A. Gundersen, et al., Cardiac myocyte excitation by ultrashort high-field pulses, Biophys. J. 96 (2009) 1640–1648. http://dx.doi.org/10.1016/j.bpj.2008.11.011.
[19] W.E. Ford, W. Ren, P.F. Blackmore, K.H. Schoenbach, S.J. Beebe, Nanosecond pulsed electric fields stimulate apoptosis without release of pro-apoptotic factors from mitochondria in B16f10 melanoma, Arch. Biochem Biophys. 497 (2010) 82–89. http://dx.doi.org/10.1016/j.abb.2010.03.008.
[20] H.T. Beier, C.C. Roth, G.P. Tolstykh, B.L. Ibey, Resolving the spatial kinetics of electric pulse-induced ion release, Biochem Biophys. Res. Commun. 423 (2012) 863–866.
[21] G.P. Tolstykh, H.T. Beier, C.C. Roth, G.L. Thompson, B.L. Ibey, 600 ns pulse electric field-induced phosphatidylinositol4,5-bisphosphate depletion, Bioelectrochemistry 100 (2014) 80–87. http://dx.doi.org/10.1016/j.bioelechem.2014.01.006.
[22] G.P. Tolstykh, H.T. Beier, C.C. Roth, G.L. Thompson, J.A. Payne, et al., Activation of intracellular phosphoinositide signaling after a single 600 ns electric pulse, Bioelectrochemistry 94 (2013) 23–29. http://dx.doi.org/10.1016/j.bioelechem.2013.05.002.
[23] G.P. Tolstykh , M, Tarango , C.C. Roth , B.L. Ibey, Dose dependent translocations of fluorescent probes of PIP2 hydrolysis in cells exposed to nanosecond pulsed electric fields. SPIE BiOS. pp. 89411T–89411T, 2014.
[24] O.N. Pakhomova, V.A. Khorokhorina, A.M. Bowman, R. Rodaite-Rivsevivciene,

G. Saulis, et al., Oxidative effects of nanosecond pulsed electric field exposure in cells and cell-free media, Arch. Biochem. Biophys. 527 (2012) 55–64.
[25] W. Ren, S.J. Beebe, An apoptosis targeted stimulus with nanosecond pulsed electric fields (nsPEFs) in E4 squamous cell carcinoma, Apoptosis 16 (2011) 382–393.
[26] K. Walker, O.N. Pakhomova, J. Kolb, K.S. Schoenbach, B.E. Stuck, et al., Oxygen enhances lethal effect of high-intensity, ultrashort electrical pulses, Bioelectromagnetics 27 (2006) 221–225.
[27] J.C. Ullery, M. Tarango, C.C. Roth, B.L. Ibey, Activation of autophagy in response to nanosecond pulsed electric field exposure, Biochem Biophys. Res. Commun. 458 (2015) 411–417. http://dx.doi.org/10.1016/j.bbrc.2015.01.131.
[28] C. Huang, K. Miyazaki, S. Akaishi, A. Watanabe, H. Hyakusoku, et al., Biological effects of cellular stretch on human dermal fibroblasts, J. Plast., Reconstr. Aesthet. Surg. 66 (2013) e351–e361.
[29] Wang JH-C, B.P. Thampatty, An introductory review of cell mechanobiology, Biomech. Model. Mechanobiol. 5 (2006) 1–16.
[30] Wang JH-C, B.P. Thampatty, J.-S. Lin, H.-J. Im, Mechanoregulation of gene expression in fibroblasts, Gene 391 (2007) 1–15.
[31] C.C. Roth, R.D. Glickman, G.P. Tolstykh, L.E. Estlack, E.K. Moen, et al., Evaluation of the genetic response of U937 and jurkat cells to 10-nanosecond electrical pulses (nsEP), PLoS One 11 (2016) e0154555.
[32] G.J. Wilmink, Using optical imaging methods to assess laser-tissue interactions (Dissertation), Vanderbilt University, 2007.
[33] J.F. Kolb, S. Kono, K.H. Schoenbach, Nanosecond pulsed electric field generators for the study of subcellular effects, Bioelectromagnetics 27 (2006) 172–187. http://dx.doi.org/10.1002/bem.20185.
[34] B.L. Ibey, C.C. Roth, A.G. Pakhomov, J.A. Bernhard, G.J. Wilmink, et al., Dose-dependent thresholds of 10-ns electric pulse induced plasma membrane disruption and cytotoxicity in multiple cell lines, PLoS One 6 (2011) e15642.
[35] C.C. Roth, R.A. Barnes Jr, B.L. Ibey, H.T. Beier, L.C. Mimun, et al., Characterization of pressure transients generated by nanosecond electrical pulse (nsEP) exposure, Sci. Rep. (2015) 5.
[36] J.L. Compton, J.C. Luo, H. Ma, E. Botvinick, V. Venugopalan, High-throughput optical screening of cellular mechanotransduction, Nat. Photonics 8 (2014) 710–715.
[37] N. Batra, S. Burra, A.J. Siller-Jackson, S. Gu, X. Xia, et al., Mechanical stress-activated integrin α5β1 induces opening of connexin 43 hemichannels, Proc. Natl. Acad. Sci. USA 109 (2012) 3359–3364.
[38] T.D. Ross, B.G. Coon, S. Yun, N. Baeyens, K. Tanaka, et al., Integrins in mechanotransduction, Curr. Opin. Cell Biol. 25 (2013) 613–618.
[39] B. Sinha, D. Köster, R. Ruez, P. Gonnord, M. Bastiani, et al., Cells respond to mechanical stress by rapid disassembly of caveolae, Cell 144 (2011) 402–413.
[40] W. Zhang, P. Wei, Y. Chen, L. Yang, C. Jiang, et al., Down-regulated expression of vimentin induced by mechanical stress in fibroblasts derived from patients with ossification of the posterior longitudinal ligament, Eur. Spine J. (2014). http://dx.doi.org/10.1007/s00586-014-3394-8.
[41] R.M. Adam, S.H. Eaton, C. Estrada, A. Nimgaonkar, S.-C. Shih, et al., Mechanical stretch is a highly selective regulator of gene expression in human bladder smooth muscle cells, Physiol. Genom. 20 (2004) 36–44.
[42] B.P. Chen, Y. Li, Y. Zhao, K. Chen, S. Li, et al., DNA microarray analysis of gene expression in endothelial cells in response to 24-h shear stress, Physiol. Genom. 7 (2002) 55–96.
[43] W. Cui, M.R. Bryant, P.M. Sweet, P.J. McDonnell, Changes in gene expression in response to mechanical strain in human scleral fibroblasts, Exp. Eye Res. 78 (2004) 275–284.
[44] R. De Araujo, Y. Oba, K. Moriyama, Identification of genes related to mechanical stress in human periodontal ligament cells using microarray analysis, J. Periodontal Res. 42 (2007) 15–22.
[45] C.W. Ward, B.L. Prosser, W.J. Lederer, Mechanical stretch induced activation of ROS/RNS signaling in striated muscle, Antioxid. Redox Signal (2013). http://dx.doi.org/10.1089/ars.2013.5517.
[46] C.P. Soves, J.D. Miller, D.L. Begun, R.S. Taichman, K.D. Hankenson, et al., Megakaryocytes are mechanically responsive and influence osteoblast proliferation and differentiation, Bone (2014).
[47] Y.-I. Yamashita, M. Shimada, K. Tachibana, N. Harimoto, E. Tsujita, et al., In vivo gene transfer into muscle via electro-sonoporation, Hum. Gene Ther. 13 (2002) 2079–2084.
[48] S. Bandoh, T. Tsukada, K. Maruyama, N. Ohkura, K. Yamaguchi, Mechanical agitation induces gene expression of NOR-1 and its closely related orphan nuclear receptors in leukemic cell lines, Leukemia 11 (1997) 1453–1458.
[49] X. Soto, J. Li, R. Lea, E. Dubaissi, N. Papalopulu, Inositol kinase and its product accelerate wound healing by modulating calcium levels, Rho GTPases, and F-actin assembly, Proc. Natl. Acad. Sci. USA 110 (2013) 11029–11034.
[50] P.S. Pardo, J.S. Mohamed, M.A. Lopez, A.M. Boriek, Induction of Sirt1 by mechanical stretch of skeletal muscle through the early response factor EGR1 triggers an antioxidative response, J. Biol. Chem. 286 (2011) 2559–2566.